cosmetics

MDPI

Article

Performance of *Platycladus orientalis* Leaves Yeast Fermented Solution on Human Dermal Papilla Cells

Kuan Chang [1], Lingjuan Liu [1], Xianqi Chen [1], Jinhua Li [1], Timson Chen [2], Zhizhen Li [2], Ya Chen [2], Ling Ma [2,*] and Jing Wang [1,*]

[1] Key Laboratory of Synthetic and Biological Colloids, Ministry of Education, School of Chemical and Material Engineering, Jiangnan University, Wuxi 214122, China
[2] Adolph Innovation Laboratory, Guangzhou AOGU Cosmetics Co., Ltd., Guangzhou 510520, China
* Correspondence: maling@adolph.cn (L.M.); jingwang@jiangnan.edu.cn (J.W.)

Abstract

Platycladus orientalis exhibits significant potential as an antioxidant, anti-inflammatory, and hair growth-promoting ingredient, while the low bioavailability of raw *Platycladus orientalis* leaves extracts limits their further application. In this study, yeast fermentation was employed to prepare *Platycladus orientalis* Leaves Yeast Fermented Solution (PYFS). Its performance on human dermal papilla cells (HDPCs) was systematically investigated. The optimal fermentation strain was screened using the methyl thiazolyl tetrazolium (MTT) assay, and *Saccharomycopsis fibuligera* CICC33226 (SF) was identified as the most suitable strain for fermentation. The effects of PYFS on the cell cycle distribution, growth factors, inflammatory factors of HDPCs, as well as its hair growth-promoting mechanism, were investigated. Experiments revealed that after fermentation, the proportion of cells in the G0/G1 phase decreased by 11.09%, while the proportion of cells in the S phase increased by 35.44%. Additionally, the level of the growth factor VEGF increased by 42.34%, while the level of the inflammatory factor TGF-β1 decreased by 23.81%. Moreover, the fermentation process correlates with altered mRNA expression of Wnt/β-catenin pathway-related genes by upregulating the mRNA expression levels of β-catenin, DVL1, and LEF1, and downregulating the mRNA expression level of DKK-1. Finally, non-targeted metabolomics technology was used to analyze the metabolite changes after fermentation. The most significant differential metabolites mainly include flavonoids, amino acids and their derivatives, and organic acids and their derivatives. This study utilized microbial fermentation technology to prepare the yeast fermentation solution, selected the optimal fermentation strain, and demonstrated that its fermentation product significantly promotes HDPC metabolic activity, supports hair follicle health by regulating the balance of growth factors, alters expression patterns of Wnt/β-catenin pathway-related genes, and substantially alters the metabolite composition of *Platycladus orientalis* leaves extract through fermentation.

Keywords: *Platycladus orientalis*; human dermal papilla cells; yeast fermentation; cell cycle

Check for updates

Academic Editor: Enzo Berardesca

Received: 10 December 2025
Revised: 3 January 2026
Accepted: 10 January 2026
Published: 12 January 2026

Copyright: © 2026 by the authors. Licensee MDPI, Basel, Switzerland. This article is an open access article distributed under the terms and conditions of the Creative Commons Attribution (CC BY) license.

1. Introduction

With the rapid development of economy and technology in modern society, there has been a growing concern regarding hair loss [1]. In recent years, the demographic affected by hair loss has been showing a trend of younger age groups, which may be related to mental stress [2,3]. Hair loss not only impacts people's aesthetic appearance but also poses a series of difficulties in their lives and work [4,5]. Numerous researchers in medical and

cosmetic community have been devoting themselves into the pathogenesis and treatment strategies of hair loss, and a variety of raw materials with anti-hair loss and hair growth properties have emerged [6].

Hair growth is intricately connected to the health of hair follicles, whose state primarily relies on the proliferation and differentiation capabilities of HDPCs [7]. Currently, drugs such as minoxidil, finasteride and spironolactone are widely used for hair loss treatment, especially for androgenetic alopecia [8]. Research has indicated that minoxidil exhibits certain performance and safety in the treatment of androgenetic alopecia, alopecia areata, and other related conditions. However, the therapeutic outcomes for a considerable number of patients remain suboptimal. Finasteride, another common medication for androgenetic alopecia, may cause some adverse reactions during long-term oral administration. Spironolactone can inhibit the production of androgens and their effects within hair follicles, thereby retarding the progression of hair loss. Nevertheless, it may be associated with side effects such as hypotension, hyperkalemia, and in some cases, urticaria and sexual dysfunction. In summary, while some drugs have been used to address hair loss in humans, they may potentially have detrimental effects on other organs [9].

In recent years, natural plant extracts a research hotspot in anti-hair loss and hair growth promotion due to their abundant bioactive components and fewer side effects [10]. Investigators have demonstrated that the *Psidium guajava* leaf extract promotes hair regrowth by scavenging free radicals and down-regulation of 5α-reductase isoenzyme expression, showing great potential for the chemoprevention and chemomodulation of androgenetic alopecia (AGA) [11]. Saw et al. reported that supercritical CO_2-extracted Angelica sinensis lipophilic extract promoted hair growth by suppressing pro-inflammatory cytokines (TNF-α, IL-1β) and activating the Nrf2/ARE pathway to upregulate antioxidant genes (Nrf2, NQO1, SOD1), restoring follicular immune homeostasis and promoting the anagen phase [12]. *Platycladus orientalis* leaves, a traditional Chinese medicinal herb, possess antioxidant, anti-inflammatory, and hair growth-promoting properties. Fu et al. found that the water extract of *Platycladus orientalis* leaves may promote hair growth by regulating the proliferation and migration of HDPCs through modulating the Akt/GSK3β/β-Catenin signaling pathway [13]. Kim et al. revealed that the leaves extract of *Platycladus orientalis* can promote hair growth by enhancing the proliferation of HDPCs by activating the non-receptor tyrosine kinase ACK1 and modulating the Wnt/β-catenin signaling pathway [14]. However, the further application of these plant-based raw materials is limited by their relatively low efficiency.

Recently, microbial fermentation has become a promising technology to enhance the biofunctions and bioavailability of various plant extracts as it can convert macromolecular substances into smaller, more skin-absorbable active components. Gao et al. used *Bacillus subtilis* to ferment soybean protein substrates, increasing methionine by 226-fold, essential amino acids to 54.48–77.12%, antioxidant and antihypertensive activities by over 60%, and spermidine content to over 40 mg/L, thereby enhancing nutritional value and bioactivity without producing toxic histamine [15]. Li et al. fermented *Polianthes tuberosa* L. flower extract with *Rhodosporidium toruloides*, finding total phenols and flavonoids doubled, DPPH and ABTS radical scavenging rates reached 47.59% and 89.87%, thereby enhancing antioxidant and multiple bioactivities [16]. Šelo et al. enhanced grape pomace nutrients and phenolics via *Trametes versicolor* solid-state fermentation, promoting its valorization and opened up avenues for its potential applications in the food industry, cosmetics industry, and other sectors [17].

In this study, yeast fermentation technology was utilized to prepare PYFS. Yeast strains were screened and compared via MTT assays. The effects of PYFS on cell cycle distribution, growth factors, and inflammatory factors of HDPCs were studied. The molecular

mechanism of regulating Wnt/β-catenin signaling pathway was further elucidated. Finally, untargeted metabolomics technology was employed to analyze metabolite changes after fermentation. By identifying key differential metabolites, the dynamic patterns of metabolite alterations during the fermentation process were revealed.

2. Materials and Methods

2.1. Materials

Platycladus orientalis leaves powder (Yuguang Yuyanfang Chinese Herbal Medicine Co., Ltd., Anguo); *Saccharomycopsis fibuligera* RTNY119002 (SF), *Candida krusei* RTNY119007 (CK), *Saccharomycopsis fibuligera* CICC33226 (SF), *Saccharomyces cerevisiae* CICC1210 (SC) were purchased from China Center of Industrial Culture Collection (Beijing, China), *Candida krusei* BNCC186835 (CK) was purchased from BeNa Culture Collection (Shangcheng, China.); HDPCs (HDPCs were purchased from Wuxi Newgain Biotechnology Co., Ltd. (Wuxi, China); Human VEGF ELISA Kit, Human TGF-β1 ELISA Kit, and Human IL-6 ELISA Kit (Shanghai Universal Biotech Co., Ltd., Shanghai, China); Cell Cycle Kit (Shanghai Beyotime Biotechnology Co., Ltd., Shanghai, China); reverse transcription kit, qPCR-related primers, and qPCR Fluorescence Quantitation Kit (Wuhan Servicebio Technology Co., Ltd., Wuhan, China); yeast extract (Thermo Fisher Scientific HyClone, Waltham, MA, USA); peptone (Beijing Aoboxing Universeen Bio-tech Co., Ltd., Beijing, China); glucose (Shanghai Macklin Biochemical Technology Co., Ltd., Shanghai, China); minoxidil (Shanghai Titan Scientific Co., Ltd., Shanghai, China); Dulbecco's modified Eagle medium (DMEM) and 0.25% trypsin (Gibco Life Technologies, Grand Island, NY, USA); phosphate-buffered saline (PBS) and penicillin-streptomycin (Thermo Fisher Scientific HyClone, Waltham, MA, USA); MTT (Sigma-Aldrich Corporation, St. Louis, MO, USA).

2.2. Preparation of PYFS

The fermentation medium was prepared by suspending 10 g of *Platycladus orientalis* leaves powder, 1 g of yeast extract, 2 g of peptone, and 2 g of glucose in 100 mL of water, followed by high-pressure sterilization (Shanghai Boxun Medical Biological Instrument Co., Ltd., Shanghai, China) at 115 °C for 20 min. Preserved yeast strains were inoculated into a liquid medium (10 g/L yeast extract, 20 g/L peptone, 20 g/L glucose) and cultured with shaking at 30 °C and 220 rpm for 24 h to fully activate the yeast and reach the logarithmic growth phase. Subsequently, the activated yeast seed culture was inoculated into the aforementioned fermentation medium at an inoculation volume of 5% (v/v). Fermentation was conducted in a constant temperature shaker (Shanghai Zhichu General Equipment Development Co., Ltd., Shanghai, China) at 30 °C and 220 rpm for 24 h. After fermentation, the broth was centrifuged at 8000 rpm for 5 min to separate the biomass from the fermentation supernatant. The supernatant was collected and filtered through a 0.22 μm microporous membrane to remove residual biomass and other insoluble impurities, yielding a clarified PYFS product.

2.3. MTT Assay for HDPCs Proliferation Rate

Cells were retrieved from liquid nitrogen, resuscitated, and cultured. At a density of 1.0×10^5 cells/mL, 100 μL of the cell suspension was seeded into each well of a 96-well cell culture plate and incubated in a cell culture incubator (Wuxi Kaipikes Technology Co., Ltd., Wuxi, China) for 24 h to allow cell adhesion and growth. For the sample groups, different mass concentrations of PYFS were added; the blank group received only DMEM (without fermentation broth). Each experimental group was set up with 5 replicate wells, followed by incubation for 24 h. After incubation, the supernatant was discarded, and 100 μL of freshly prepared MTT solution (0.5 mg/mL) was added to each well, with subsequent incubation for 4 h. The MTT solution was then removed, and 100 μL of dimethyl sulfoxide

(DMSO) was added to each well. The plate was shaken for 5 min to dissolve the formazan crystals at the bottom of the wells. Finally, the optical density (OD) value was measured at a wavelength of 490 nm. And the experiment was independently conducted 3 times as biological replicates. The cell proliferation rate was calculated using the following formula:

$$cell\ proliferation(\%) = \frac{sample\ group\ OD\ value}{blank\ group\ OD\ value} \times 100 \quad (1)$$

2.4. PI Staining for Cell Cycle Analysis

Cell culture was performed as described in Section 2.3. Cells were seeded at a density of 3.0×10^5 cells/mL (2 mL per well) in 6-well cell culture plates and cultured for 24 h to allow cell adhesion. Three experimental groups were established: the blank group, 5 μg/mL minoxidil (this concentration effectively promotes HDPC proliferation and cell cycle progression [8,10]) positive control group, and PYFS sample group. Cells were cultured for an additional 24 h. For detection, cells were trypsinized, centrifuged at 1000× *g* for 5 min, and the supernatant was discarded. The cells were washed twice with pre-cooled PBS (centrifuged at 1000× *g* for 5 min, supernatant discarded) and fixed with pre-cooled 70% ethanol at 4 °C for 12 h. Cells were then washed once with PBS to remove residual ethanol. Pre-configured propidium iodide (PI) staining solution was added, and the cells were resuspended by pipetting. After incubation in the dark at 37 °C for 30 min, the cells were analyzed by flow cytometry. The Proliferation Index was calculated using the following formula:

$$Proliferation\ Index(\%) = \frac{S + (G2 + M)}{(G0 + G1) + S + (G2 + M)} \times 100 \quad (2)$$

In the formula, (G0 + G1) represents the proportion of diploid cells, S denotes the proportion of cells in the DNA synthesis phase, and (G2 + M) indicates the proportion of tetraploid cells.

2.5. ELISA for VEGF, TGF-β1, and IL-6 Levels

Cell culture was performed as described in Section 2.3, and cells were seeded into three 96-well plates. For the first plate, the blank group, 5 μg/mL minoxidil positive control group, and PYFS sample group were established. Cells incubate for 24 h, and the levels of VEGF and TGF-β1 in the cell supernatant were measured according to the ELISA kit instructions, with three replicates per group. For the second plate, different concentration gradients of DHT solution were added to establish a DHT-induced stimulation model. For the third plate, the following groups were set up: blank group, DHT model group, DHT + 5 μg/mL minoxidil co-culture positive control group, and DHT + PYFS co-cultured sample group. Corresponding reagents were added, and incubation was continued for 24 h. Subsequently, the IL-6 level in the cell supernatant was measured according to the ELISA kit instructions, and the experiment was repeated 3 times as biological replicates.

2.6. Total RNA Extraction and RT-qPCR Detection

A similar procedure to that described in Section 2.3 was used. Cells were seeded at a density of 3.0×10^5 cells/mL (2 mL per well) in 6-well cell culture plates and cultured for 24 h to allow cell adhesion. The blank group, 5 μg/mL minoxidil positive control group, and PYFS sample group were established, and cells were cultured for an additional 24 h. The supernatant was removed, and cells were washed twice with PBS. Subsequently, 1 mL of Trizol reagent was added, and the mixture was allowed to stand for 2 min. Cells were disrupted by pipetting, followed by the addition of 250 μL of chloroform and vortexing for 3 min. The sample was then centrifuged at 4 °C and 12,000 rpm for 10 min. The upper aqueous phase was transferred to a new centrifuge tube, and 0.8 volumes of

isopropanol were added. After incubation at room temperature for 10 min to promote RNA precipitation, centrifugation was performed at 4 °C and 12,000 rpm for 10 min. The supernatant was discarded, and the RNA pellet was collected, washed with 75% ethanol (prepared with RNase-free water), and air-dried at room temperature. The RNA pellet was dissolved in RNA dissolution buffer and adjusted to a concentration of 200 ng/μL. Complementary DNA (cDNA) was synthesized using a reverse transcription kit according to the manufacturer's protocol. Relative quantitative analysis was performed based on the cycle threshold (CT) values of each gene using the ΔΔCT method. Each group was set with 3 technical replicates, and the experiment was performed 3 times as biological replicates. Primer sequences are shown in Table 1. GAPDH was selected as the reference gene for data normalization, consistent with the methodology of previously published studies where GAPDH expression exhibited high stability under identical experimental conditions [13,14].

$$\Delta\Delta CT\ Method:$$
$$A = \mathrm{CT}(\text{Target Gene, Test Sample}) - \mathrm{CT}(\text{Reference Gene, Test Sample})$$
$$B = \mathrm{CT}(\text{Target Gene, Control Sample}) - \mathrm{CT}(\text{Reference Gene, Control Sample})$$
$$K = A - B$$
$$Fold\ Change = 2^{-K}$$

Table 1. Primer Sequences.

Primer Name	Upstream Primer Sequences (5′–3′)	Downstream Primer Sequences (5′–3′)
GAPDH	GGAAGCTTGTCATCAATGGAAATC	TGATGACCCTTTTGGCTCCC
β-catenin	GCTGAAGGTGCTATCTGTCTGC	CCTTCCATCCCTTCCTGTTTAG
DVL1	TGACGGGATGGACAACGAGA	CATCCTCGTCCGAGTCCACA
LEF1	GCGAATGTCGTTGCTGAGTGTA	GCTGTCTTTCTTTCCGTGCTAA
DKK-1	TCCAACGCTATCAAGAACCTGC	ACGGGTACGGCTGGTAGTTGT

2.7. Untargeted Metabolomics Analysis of PYFS Before and After Fermentation

To investigate changes in metabolite composition, UHPLC-Q/TOF-MS was employed to analyze the fermented solution. Briefly, an appropriate amount of fermented solution was sampled and diluted as required, followed by filtering through 0.22 μm microporous membrane. The sample was then injected into an ultra-high performance liquid chromatography system (Waters Acquity UHPLC, Waters Corporation, Milford, MA, USA) equipped with an Acquity BEH C18 column (2.1 mm × 100 mm, 1.7 μm) and coupled to a quadrupole-time-of-flight tandem mass spectrometer (Waters Acquity Mass Q-TOF, Waters Corporation, Milford, MA, USA). Detailed analytical conditions are provided in the SI (Table S1).

The obtained data were subjected to missing value imputation and normalization to ensure accuracy and comparability. The metware Cloud platform (https://cloud.metware.cn/#/user/login) (accessed on 15 October 2024) was utilized for principal component analysis (PCA) and orthogonal partial least squares discriminant analysis (OPLS-DA) to reveal differences among different samples. Simultaneously, significantly differential metabolites were screened based on a combination of variable importance in projection (VIP) values, fold change (FC), and P-values from Student's *t*-test. Heatmaps were generated to visually display metabolite changes among different samples.

2.8. Data Processing and Statistical Analysis

Flow cytometry data were analyzed using FlowJo v10.8.1 software (FlowJo LLC, Ashland, OR, USA). All other experimental data were processed with GraphPad Prism 8. For multi-group comparisons, one-way analysis of variance (ANOVA) was conducted, followed by Tukey's post hoc test for pairwise comparisons. For two-group comparisons,

an independent samples *t*-test was used. * $p < 0.05$ indicates a statistically significant difference, ** $p < 0.01$ indicates a highly statistically significant difference, and *** $p < 0.001$ indicates an extremely statistically significant difference.

3. Results and Discussion

3.1. Effects of PYFS on HDPCs Viability and Cell Cycle

The effects of different PYFS samples on HDPCs viability were investigated for fermentation strain screening. Three different yeast strains (SF, CK, SC) were employed to prepare PYFS using the procedure described in Section 2.2. As shown in Figure 1, *Platycladus orientalis* leaves extract solution (PES) and three PYFS samples significantly enhanced HDPCs metabolic activity. Among them, PYFS-SF exhibited the highest proliferation rate of 152.45% (*** $p < 0.001$) at a concentration of 2.5 mg/mL. Therefore, SF was selected as the most suitable strain for fermentation and used for subsequent experiments.

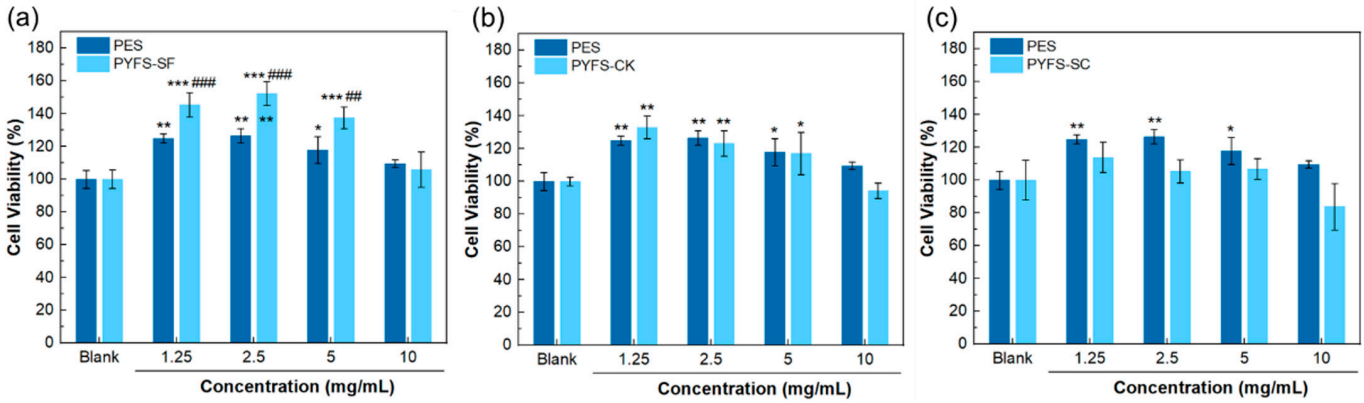


Figure 1. Effects of PES and (**a**) PYFS-SF; (**b**) PYFS-CK; (**c**) PYFS-SC on the activity of HDPCs. Data are presented as mean ± SD ($n = 3$ biological replicates). (Compared with blank group, * $p < 0.05$, ** $p < 0.01$, *** $p < 0.001$; Compared with PES, ## $p < 0.01$, ### $p < 0.001$).

Cell proliferation, the foundation to organism growth, development, and tissue repair, is typically divided into four main phases: G1 phase (pre-DNA synthesis), S phase (DNA synthesis), G2 phase (post-DNA synthesis), and M phase (cell division) [18]. Cell proliferation activity was assessed by detecting cell cycle distribution using flow cytometry (Figure 2). Proliferation index, as an important indicator reflecting the proportion of cells in the proliferative phase (S and G2/M phases) within a cell population, was calculated and listed in Table 2 [19]. As shown in Figure 2 and Table 2, compared with the blank group, PYFS-treated cells exhibited a significantly reduced proportion in the G0/G1 phase (**$p < 0.01$), while the proportions of cells in the S phase and G2/M phase significantly increased (** $p < 0.01$; * $p < 0.05$), which was similar with minoxidil group. Furthermore, compared with PES-treated cells, PYFS-SF reduced the percentage of G0/G1 phase cells by 11.09% (# $p < 0.05$) and increased the percentage of S phase cells by 35.44% (## $p < 0.01$). These percentage changes are presented relative to PES to specifically isolate the enhancement effect induced by fermentation, while comparisons to the blank group confirm the inherent biological activity of the extract. This dual comparison is critical to validating the core hypothesis of this study—that yeast fermentation improves the bioactivity of *Platycladus orientalis* leaves extract. MTT assay reflects changes in cell metabolic activity, which correlates with proliferation. This was further supported by cell cycle analysis showing increased S and G2/M phase populations, confirming enhanced cell proliferation.

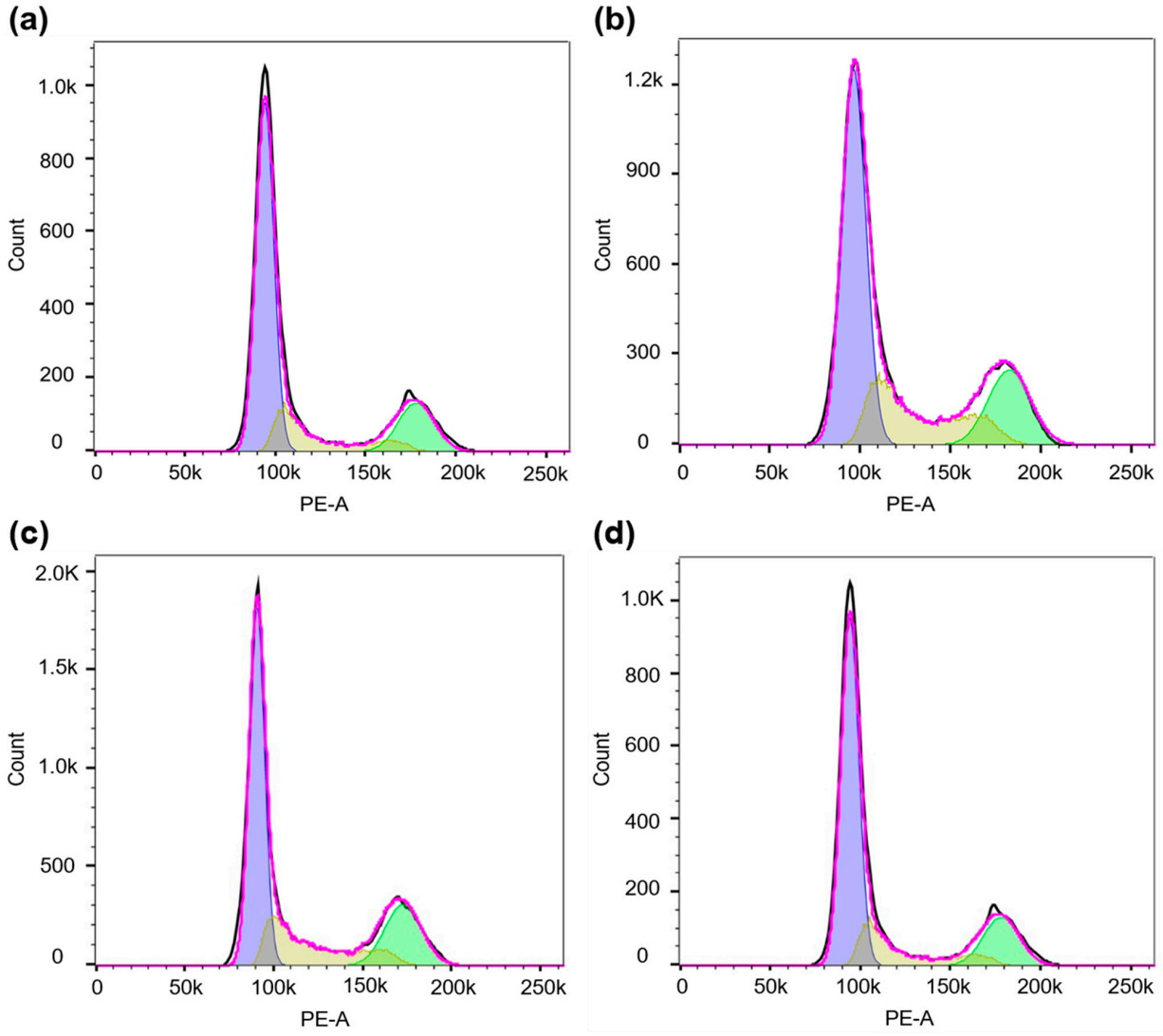


Figure 2. Statistical analysis of the proportion of cells in different cycles detected by flow cytometry. (**a**) Blank group; (**b**) Minoxidil group; (**c**) PES group; (**d**) PYFS-SF group. Data are presented as mean ± SD (n = 3 biological replicates).

Table 2. Proportion of HDPC in Each Stage of the Cell Cycle.

	G0/G1/%	S/%	G2/M/%	PI/%
Blank group	61.1	19.5	17.9	37.97%
5 μg/mL minoxidil	51.4 (**)	25.6 (*)	21.3 (*)	47.71%
2.5 mg/mL PES	53.2	23.7	18.3	44.12%
2.5 mg/mL PYFS-SF	47.3 (** #)	32.1 (** ##)	20.6 (*)	52.70%

Note: Data are presented as mean ± SD (n = 3 biological replicates). Compared with blank group, * $p < 0.05$, ** $p < 0.01$; Compared with PES, # $p < 0.05$, ## $p < 0.01$.

A key limitation is the use of HDPC monocultures, which do not recapitulate the complex in vivo microenvironment of hair follicles (e.g., interactions with keratinocytes, fibroblasts, and immune cells). While HDPCs are central to follicular homeostasis, extrapolation to in vivo hair growth requires validation in animal models (e.g., mouse dorsal skin models). Additionally, the lack of 3D co-culture systems limits insights into cell–cell communication effects, which should be addressed in future studies.

3.2. Regulatory Effect of PYFS on VEGF, TGF-β1, and IL-6 Levels

To further investigate the performance and mechanism of PYFS in regulating HDPC function, the levels of VEGF and TGF-β1 secreted by HDPCs were measured. ELISA results indicated that both PES and PYFS-SF could regulate the expression of growth factors in HDPCs, significantly upregulating VEGF levels and effectively downregulating TGF-β1 levels. As shown in Figure 3, compared with the blank group, PYFS-SF significantly increased VEGF content by 88.68% (*** $p < 0.001$) and reduced TGF-β1 content by 34.90% (** $p < 0.01$). More importantly, the 42.34% (## $p < 0.01$) upregulation of VEGF is revealed relative to PES to directly demonstrate that fermentation enhances the growth factor-regulating capacity of the original extract, beyond the baseline activity observed when compared to the blank group. Similarly, the 23.81% (# $p < 0.05$) downregulation of TGF-β1 relative to PES highlights fermentation-specific improvements in inhibiting this catagen-promoting factor. These results suggest that yeast fermentation can effectively enhance the ability of PES to regulate growth factor secretion in HDPCs, thereby promoting the proliferation and differentiation of follicular cells.

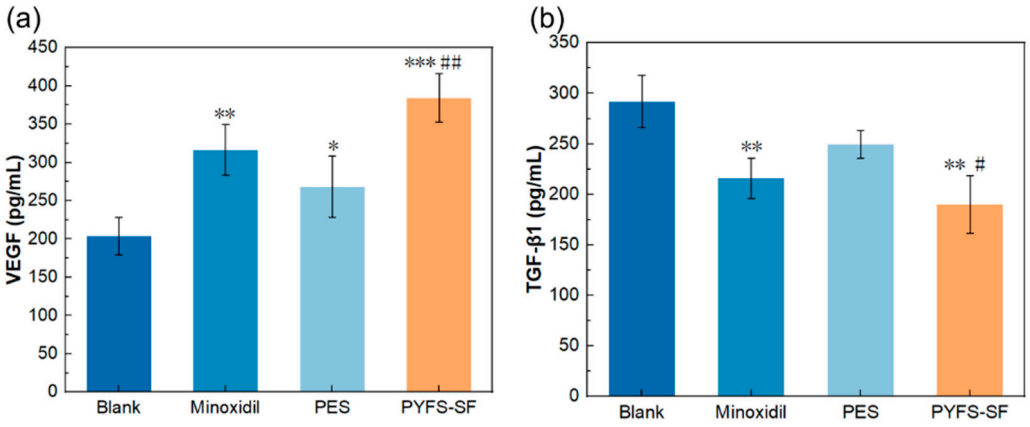


Figure 3. Effects of PES and PYFS-SF on the regulation of VEGF (**a**) and TGF-β1 (**b**) levels in HDPCs. Data are presented as mean ± SD ($n = 3$ biological replicates. (Compared with blank group, * $p < 0.05$, ** $p < 0.01$, *** $p < 0.001$; Compared with PES, # $p < 0.05$, ## $p < 0.01$).

IL-6 is a pleiotropic cytokine involved in chronic inflammation and autoantibody production, which can reduce keratinocyte activity, inhibit hair shaft elongation, and suppress the proliferation of matrix cells [20]. The performance of PYFS-SF in a DHT-induced HDPC inflammation model was investigated by evaluating the IL-6 expression level in HDPCs. As shown in Figure 4a, compared with the blank group, DHT at concentrations of 5.0 and 10.0 μg/mL significantly induced IL-6 secretion (*** $p < 0.001$). As shown in Figure 4b, when cells were co-incubated with DHT and either PES or PYFS-SF, the secreted IL-6 level decreased to a certain extent. The PYFS-SF group achieved an inhibition rate of 44.61% (### $p < 0.001$) on IL-6 secretion, which was similar to that of the minoxidil group, while the PES group exhibited partial inhibition with no statistically significant difference ($p > 0.05$). These results indicate that PYFS-SF significantly correlates with greater suppression of on DHT-induced secretion of the inflammatory cytokine IL-6.

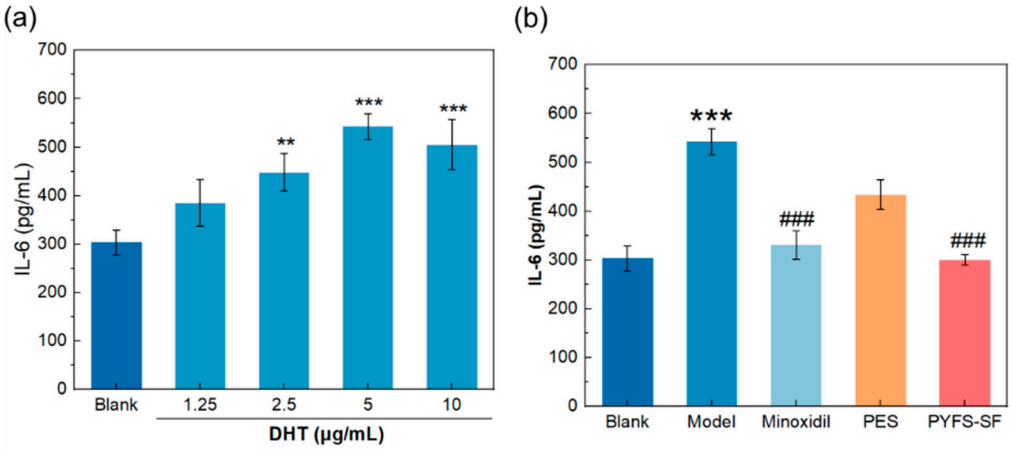


Figure 4. Effect of PES and PYFS-SF on inhibition of DHT-induced secretion of inflammatory cytokine IL-6: (**a**) Dose-dependent effect of DHT on IL-6 secretion; (**b**) Regulatory effects of PES and PYFS-SF on IL-6 levels. Data are presented as mean ± SD (n = 3 biological replicates). (Compared with blank group, ** $p < 0.01$, *** $p < 0.001$; Compared with PES, ### $p < 0.001$).

3.3. Effects of PYFS on the Wnt/β-Catenin Signaling Pathway in HDPCs

By regulating the secretion of growth factors to activate the Wnt/β-catenin signaling pathway, Ru et al. demonstrated that 1,3,6-tri-o-galloylglucose and Camellia oleifera seed shell polyphenols can prolong the duration of hair growth [21]. *Platycladus orientalis* leaves can promote hair growth through multiple pathways, with the Wnt/β-catenin signaling pathway being a typical example [13,14]. The Wnt/β-catenin signaling pathway is one of the key regulatory mechanisms in hair loss. Activation of Wnt/β-catenin pathway promotes follicle regeneration, maintains normal follicle cycling, and delays follicle aging, making it one of the most deeply studied and representative signaling pathways [22,23]. The regulatory effects of PES and PYFS-SF on the Wnt/β-catenin signaling pathway were investigated by examining the mRNA expression levels of key proteins (β-catenin and disheveled 1 [DVL1]), a downstream transcription factor (lymphoid enhancer-binding factor 1 [LEF1]), and a natural inhibitor (dickkopf-1 [DKK-1]) via RT-qPCR. As illustrated in Figure 5, both PES and PYFS-SF significantly upregulated the mRNA expression levels of β-catenin, DVL1, and LEF1 in HDPCs, while significantly downregulating the mRNA expression level of DKK-1. Further analysis revealed that the PYFS-SF treatment group exhibited a more significant regulatory effect on the Wnt/β-catenin signaling pathway than the PES group. Specifically, PYFS-SF upregulated the mRNA expression levels of β-catenin, DVL1, and LEF1 by 28.71% (## $p < 0.01$), 32.11% (## $p < 0.01$), and 20.13% (# $p < 0.05$), respectively, while downregulating DKK-1 mRNA expression by 40.45% (### $p < 0.001$). These results indicate that PYFS-SF modulates the mRNA expression of key genes in the Wnt/β-catenin signaling pathway, suggesting a potential regulatory role in promoting HDPC proliferation and differentiation to support hair follicle regeneration. However, confirmation of pathway activation at the protein level (e.g., total and nuclear β-catenin expression) is required in future studies.

The observed regulatory effects of PYFS-SF on the Wnt/β-catenin pathway are highly relevant to hair follicle (HF) physiology, as this pathway serves as the master regulator of HF homeostasis. During the anagen phase, nuclear accumulation of β-catenin in HDPCs forms a complex with LEF1, activating the transcription of proliferation-related genes that drive HDPC expansion and HF elongation [22,23]. In contrast, the pathway antagonist DKK-1 promotes β-catenin degradation, triggering the transition to the regression phase [8]. PYFS-SF-mediated upregulation of β-catenin, DVL1, and LEF1, coupled with downregulation of DKK-1, directly sustains the anagen phase—addressing a key pathological feature of

androgenetic alopecia (AGA), where impaired Wnt/β-catenin signaling leads to premature HF miniaturization [14]. Additionally, the growth factors and inflammatory cytokines regulated by PYFS-SF (VEGF, TGF-β1, IL-6) further modulate HF dynamics: VEGF induces angiogenesis around the dermal papilla to ensure nutrient supply, excessive TGF-β1 triggers HF regression, and IL-6 mediates androgen-induced hair loss [20]. Collectively, these findings demonstrate that PYFS-SF exerts pro-hair effects by reactivating the anagen-promoting Wnt/β-catenin pathway and restoring the balance of growth factors/cytokines, all of which are central to maintaining HF physiological function.

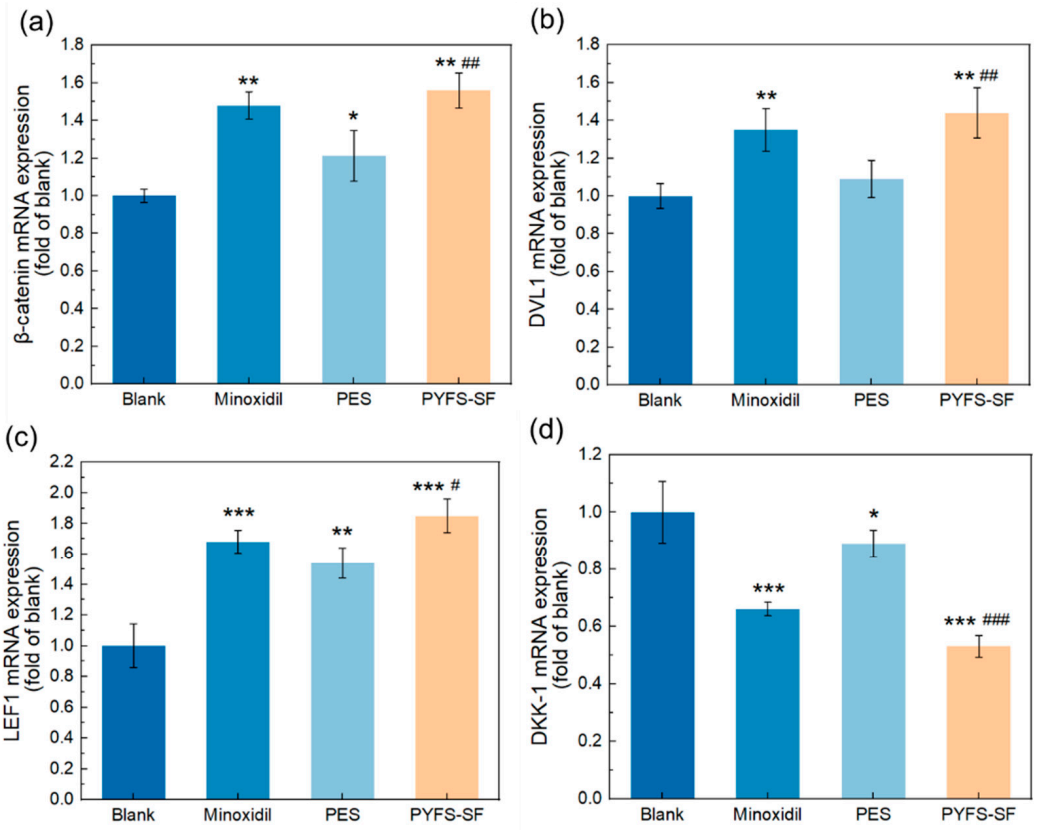


Figure 5. Effects of PES and PYFS-SF on the regulation of (**a**) β-catenin, (**b**) DVL1, (**c**) LEF1 and (**d**) DKK-1 mRNA expression in the Wnt/β-catenin signaling pathway. Data are presented as mean ± SD (n = 3 biological replicates). (Compared with blank group, * $p < 0.05$, ** $p < 0.01$, *** $p < 0.001$; Compared with PES, # $p < 0.05$, ## $p < 0.01$, ### $p < 0.001$).

3.4. Changes in Metabolites of PYFS-SF Before and After Fermentation

To assess component differences between the PES and PYFS-SF, principal component analysis (PCA) was performed on the UHPLC-Q/TOF-MS data of both groups to observe the separation trend and distribution of sample points. In Figure 6, Group A represents PES and group B represents PYFS-SF. PCA is an unsupervised multivariate statistical analysis method that visualizes high-dimensional data through dimensionality reduction, thereby intuitively reflecting the overall differences between samples [24]. As shown in the PCA score plot, no obvious outliers were observed, and both groups exhibited good clustering. This indicates that the composition changed significantly after fermentation, forming distinct metabolic profiles with clear inter-group differences. This result laid the foundation for subsequent in-depth analysis.

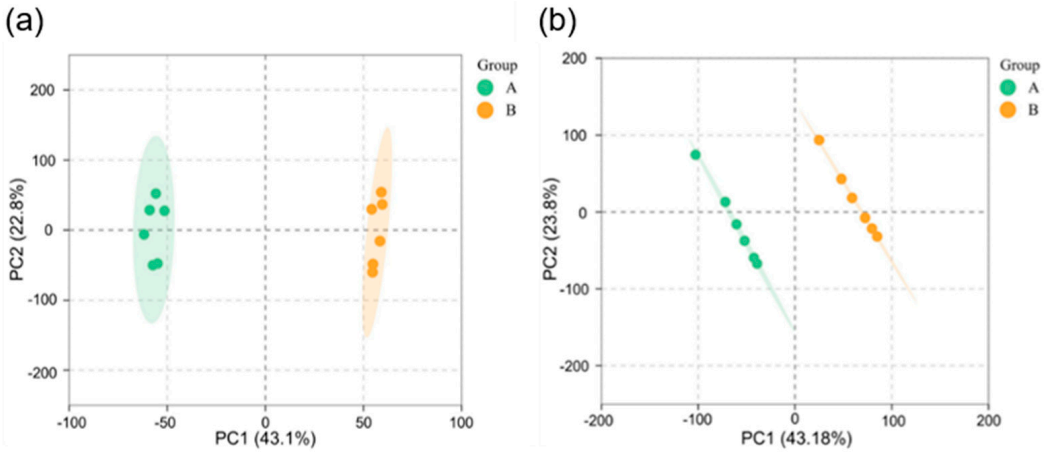


Figure 6. PCA scores of PES (Group A) and PYFS-SF (Group B) in positive ion mode (**a**) and negative ion mode (**b**).

To further verify inter-group differences and screen for potential differential metabolites, OPLS-DA analysis was conducted to explore the separation trends. The results are shown in Figure 7. Model evaluation yielded three key parameters: R^2X, R^2Y, and Q^2. Among these parameters, R^2X represents the model's explanatory power for the independent variables (metabolite data), R^2Y represents the explanatory power for the dependent variables (grouping information), and Q^2 reflects the model's predictive ability. In positive ion mode, these parameters were 0.519, 1.0, and 0.986, respectively. In negative ion mode, they were 0.652, 1.0, and 0.987, respectively. These results indicate that the established OPLS-DA model exhibited excellent predictive ability, reliably reflecting inter-group differences and enabling the screening of potential differential metabolites.

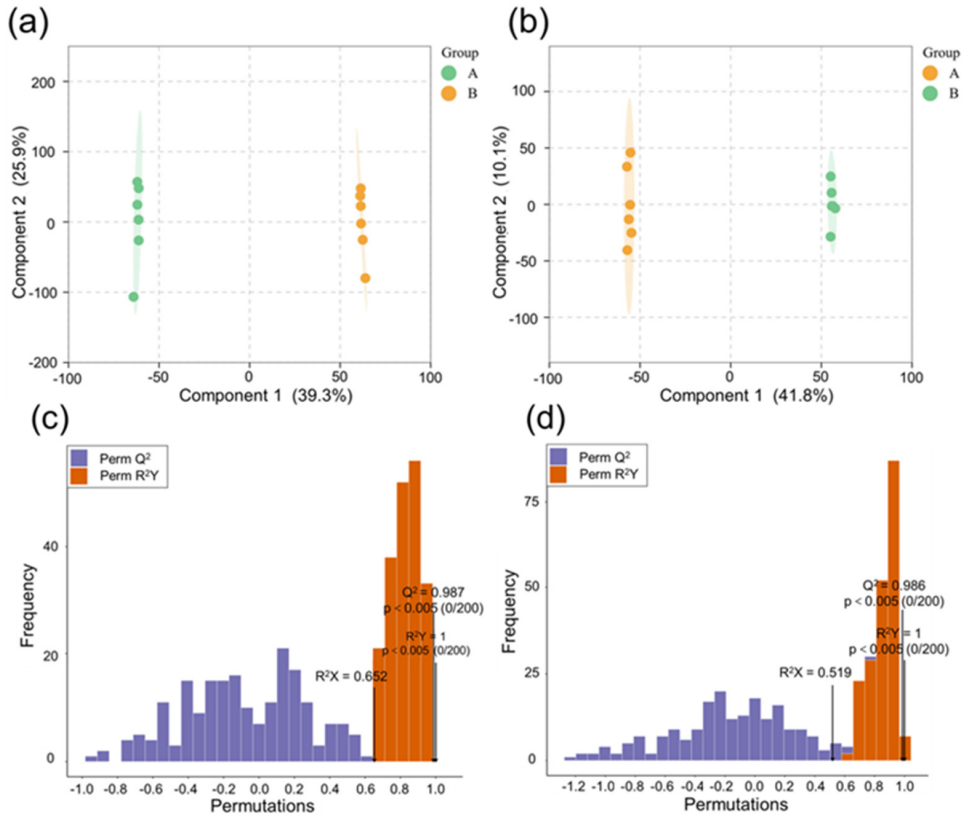


Figure 7. OPLS-DA scores and parameter graphs of PES (Group A) and PYFS-SF (Group B) in positive ion mode (**a**,**c**) and negative ion mode (**b**,**d**).

Furthermore, metabolic differences between PES and PYFS-SF were analyzed using three key parameters: VIP, fold change (FC), and significance level (p -value). The screening thresholds were set as FC > 2, VIP > 1, and $p < 0.05$. Based on these criteria, a total of 2439 significantly differential metabolites were identified across positive and negative ion modes. Among these, 1510 metabolites exhibited significantly upregulated expression levels (with enhanced biological activity), while 929 metabolites showed a downregulated trend, suggesting their inhibition or conversion during fermentation. Subsequently, based on the volcano plot (Figure 8), the top 50 differential metabolites with the highest VIP values were selected to generate a VIP heatmap (Figure 9) and a clustered heatmap (Figure 10).

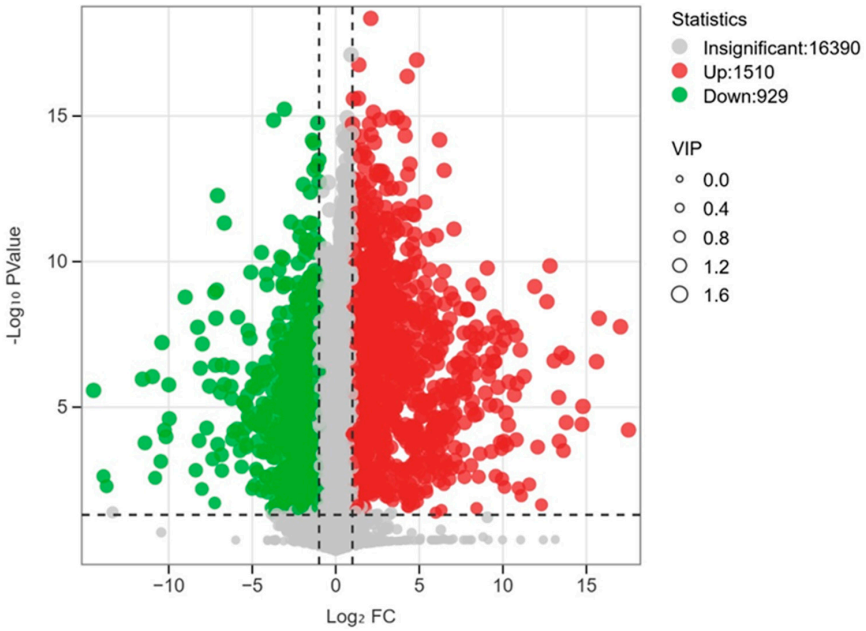


Figure 8. Volcano plot of differentially expressed metabolites between PES and PYFS-SF.

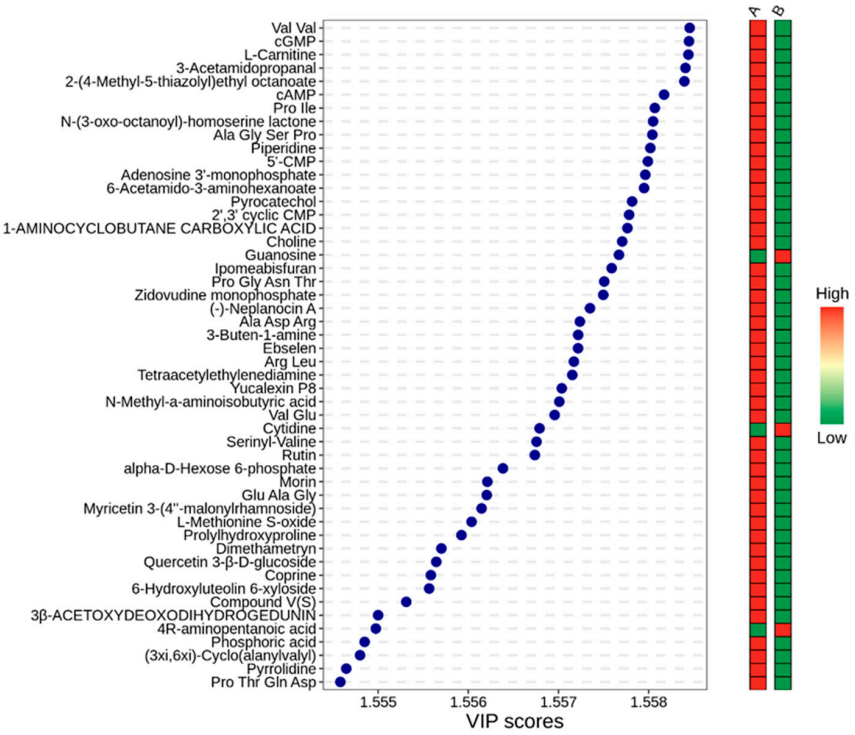


Figure 9. VIP heatmap of differentially expressed metabolites between PES and PYFS-SF.

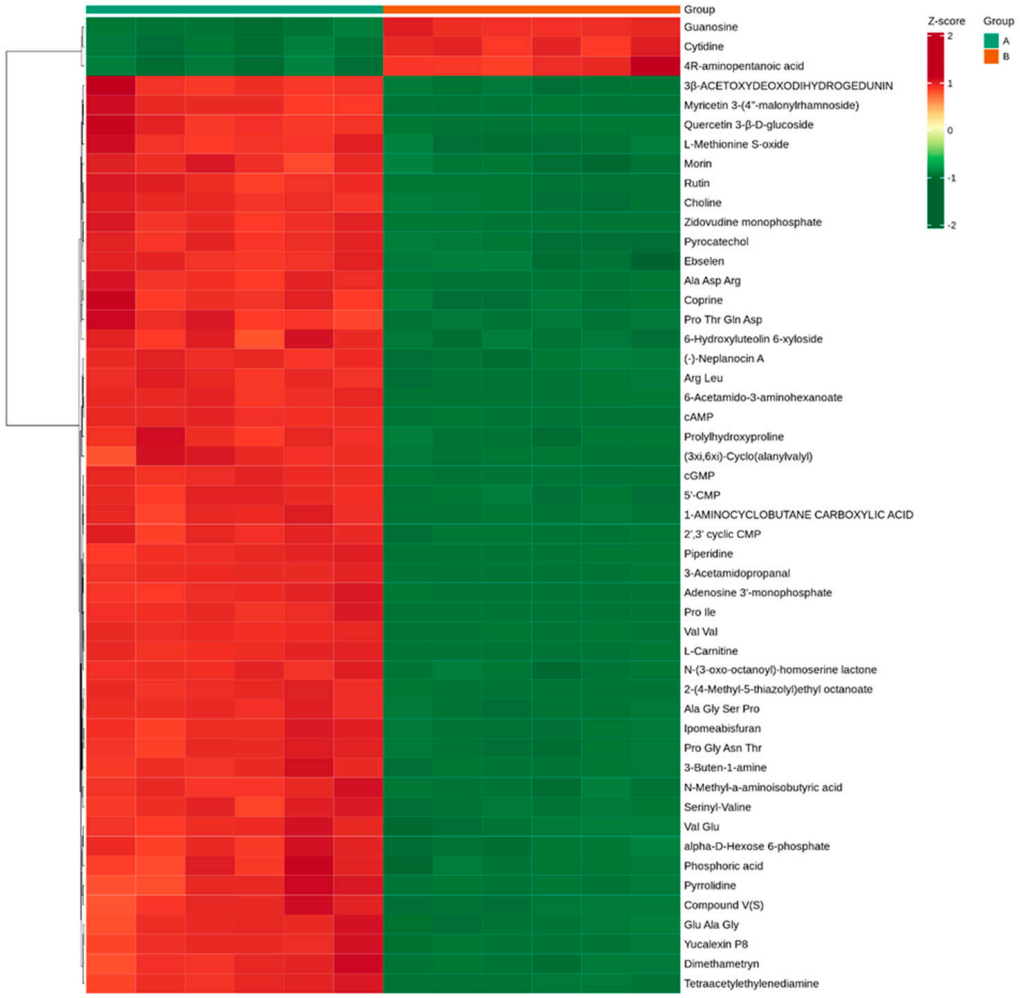


Figure 10. Heatmap of clustered metabolites with significant differences between PES and PYFS-SF.

The most significant differential metabolites mainly include flavonoids (e.g., Pyrocatechol, Morin), amino acids and their derivatives (e.g., Val Val, L-Carnitine), and organic acids and their derivatives. The screening and identification of these key metabolites provide important clues for further revealing the metabolic differences between PES and PYFS-SF, and lay a theoretical foundation for optimizing fermentation processes and developing functional metabolites. Among these differential metabolites, two key bioactive compounds were prioritized for functional annotation: Pyrocatechol (a flavonoid derivative): With a VIP value of 1.558, FC of 3.21, and $p < 0.01$, it was significantly upregulated in PYFS-SF. Pyrocatechol has been well-documented for its potent anti-inflammatory activity by inhibiting the secretion of pro-inflammatory cytokines such as IL-6, which aligns with our ELISA results showing that PYFS-SF strongly suppressed DHT-induced IL-6 production in HDPCs. L-carnitine (an amino acid derivative): It exhibited a VIP value of 1.558, FC of 2.87, and $p < 0.01$. As a key mediator of mitochondrial energy metabolism, L-carnitine enhances cell metabolic activity and proliferation, which is consistent with our MTT and cell cycle data demonstrating improved HDPC metabolic activity and increased S phase population upon PYFS-SF treatment.

These findings link specific fermentation-induced metabolic changes to the observed biological effects, reinforcing that the enhanced bioactivity of PYFS-SF is attributed to the accumulation of functionally relevant metabolites. Flavonoids possess biological activities such as antioxidant, anti-inflammatory, and antibacterial properties, whose levels may be associated with enzymatic reactions or substrate conversion during fermenta-

tion [25,26]. Amino acids and their derivatives play important roles in protein synthesis and energy metabolism, and their changes may reflect microbial metabolic activity during fermentation [27,28]. Organic acids and their derivatives are crucial in energy metabolism and intermediary metabolism; their changes may be relate to substrate utilization and product accumulation during fermentation [29]. Collectively, these findings offer crucial insights into the metabolic discrepancies between PES and PYFS-SF, and establish a theoretical basis for the optimization of fermentation technologies and the exploitation of functional metabolites.

4. Conclusions

In this study, yeast fermentation was employed to prepare PYFS using SF strain. Experimental results showed that 2.5 mg/mL PYFS-SF increased the proliferation rate of HDPCs by 152.45%, significantly outperforming unfermented PES, and reduced the percentage of cells in the G0/G1 phase by 11.09%, while increasing that in S phase by 35.44%. PYFS-SF upregulated VEGF levels by 42.34%, downregulated TGF-β1 levels by 23.81%, and downregulated IL-6 levels by 44.61%, indicating promotions in the proliferation and differentiation of hair follicle cells and inhibition on inflammatory responses. PYFS-SF is associated with altered expression of Wnt/β-catenin pathway-related genes: β-catenin, DVL1, and LEF1 mRNA levels are upregulated by 28.71%, 32.11%, and 20.13%, respectively, while DKK-1 mRNA is downregulated by 40.45%. These performances could be ascribed to the enhancement of active components including flavonoids, amino acid derivatives and organic acids after fermentation, as suggested by the non-targeted metabolomics before and. This study reveals the mechanism of action of PYFS-SF on HDPCs, validate the fermentation-enhanced bioactivity.

Supplementary Materials: The following supporting information can be downloaded at: https://www.mdpi.com/article/10.3390/cosmetics13010014/s1. Table S1: UHPLC-Q/TOF-MS Chromatographic Gradient Elution Method and Mass Spectrometry Parameters for Cell Metabolite Analysis.

Author Contributions: Conceptualization, J.W., J.L., T.C., Z.L. and K.C.; methodology, X.C. and Y.C.; investigation, J.W., L.M. and K.C.; resources, T.C., Z.L. and Y.C.; data curation, J.W. and K.C.; writing—original draft preparation, L.L.; writing—review and editing, J.W. and K.C. All authors have read and agreed to the published version of the manuscript.

Funding: This research received no external funding.

Institutional Review Board Statement: Not applicable.

Informed Consent Statement: Not applicable.

Data Availability Statement: The data presented in this study are available on request from the corresponding author.

Conflicts of Interest: Authors Timson Chen, Zhizhen Li, Ya Chen, Ling Ma were employed by the Adolph Innovation Laboratory, Guangzhou AOGU Cosmetics Co., Ltd. The remaining authors declare that the research was conducted in the absence of any commercial or financial relationships that could be construed as potential conflicts of interest. The funders had no role in the design of the study; in the collection, analyses or interpretation of data; in the writing of the manuscript; or in the decision to publish the results.

References

1. Cash, T.F. The Psychosocial Consequences of Androgenetic Alopecia: A Review of the Research Literature. *Br. J. Dermatol.* **1999**, *141*, 398–405. [CrossRef]
2. Liang, W.; Zhao, Y.; Cai, B.; Huang, Y.; Chen, X.; Ni, N.; Wang, Y.; Lin, Z.; Lin, C.; Huang, K. Psychological Stress Induces Hair Regenerative Disorders through Corticotropin-Releasing Hormone-Mediated Autophagy Inhibition. *Biochem. Biophys. Res. Commun.* **2024**, *699*, 149564. [CrossRef]
3. Malta, M.; Corso, G. Understanding the Association Between Mental Health and Hair Loss. *Cureus* **2025**, *17*, e84777. [CrossRef]
4. Muntyanu, A.; Gabrielli, S.; Donovan, J.; Gooderham, M.; Guenther, L.; Hanna, S.; Lynde, C.; Prajapati, V.H.; Wiseman, M.; Netchiporouk, E. The Burden of Alopecia Areata: A Scoping Review Focusing on Quality of Life, Mental Health and Work Productivity. *J. Eur. Acad. Dermatol. Venereol.* **2023**, *37*, 1490–1520. [CrossRef]
5. Al Najjar, O.A.; Alkhars, M.A.; Al Molhim, S.F.; AlAjmi, M.S.; Alhafith, A.A.; Al Najjar, M.A.; AlMaqhawi, A. The Impact of Androgenic Alopecia on the Quality of Life of Male Individuals: A Cross-Sectional Study. *Cureus* **2023**, *15*, e47760. [CrossRef] [PubMed]
6. Xu, J.; He, C.; Tian, R. Screening of Anti-Hair Loss Plant Raw Materials Based on Reverse Network Pharmacology and Experimental Validation. *Curr. Issues Mol. Biol.* **2025**, *47*, 68. [CrossRef]
7. Lee, J.O.; Kim, Y.; Jang, Y.N.; Lee, J.M.; Shin, K.; Jeong, S.; Chung, H.-J.; Kim, B.J. ICP5249 Promotes Hair Growth by Activating the AMPK-Autophagy Signaling Pathway. *J. Microbiol. Biotechnol.* **2024**, *34*, 1810–1818. [CrossRef] [PubMed]
8. Desai, D.D.; Nohria, A.; Sikora, M.; Anyanwu, N.; Shapiro, J.; Lo Sicco, K.I. Comparative Analysis of Low-Dose Oral Minoxidil with Spironolactone Versus Finasteride or Dutasteride in Female Androgenetic Alopecia Management. *Arch. Dermatol. Res.* **2024**, *316*, 622. [CrossRef] [PubMed]
9. Greenblatt, D.J. Adverse Reactions to Spironolactone: A Report From the Boston Collaborative Drug Surveillance Program. *JAMA* **1973**, *225*, 40. [CrossRef]
10. Choi, J.Y.; Boo, M.Y.; Boo, Y.C. Can Plant Extracts Help Prevent Hair Loss or Promote Hair Growth? A Review Comparing Their Therapeutic Efficacies, Phytochemical Components, and Modulatory Targets. *Molecules* **2024**, *29*, 2288. [CrossRef]
11. Ruksiriwanich, W.; Khantham, C.; Muangsanguan, A.; Phimolsiripol, Y.; Barba, F.J.; Sringarm, K.; Rachtanapun, P.; Jantanasakulwong, K.; Jantrawut, P.; Chittasupho, C.; et al. Guava (*Psidium guajava* L.) Leaf Extract as Bioactive Substances for Anti-Androgen and Antioxidant Activities. *Plants* **2022**, *11*, 3514. [CrossRef]
12. Saw, C.L.L.; Wu, Q.; Su, Z.; Wang, H.; Yang, Y.; Xu, X.; Huang, Y.; Khor, T.O.; Kong, A.T. Effects of Natural Phytochemicals in *Angelica Sinensis* (Danggui) on Nrf2-mediated Gene Expression of Phase II Drug Metabolizing Enzymes and Anti-inflammation. *Biopharm. Drug Dispos.* **2013**, *34*, 303–311. [CrossRef] [PubMed]
13. Fu, H.; Li, W.; Weng, Z.; Huang, Z.; Liu, J.; Mao, Q.; Ding, B. Water Extract of Cacumen Platycladi Promotes Hair Growth Through the Akt/GSK3β/β-Catenin Signaling Pathway. *Front. Pharmacol.* **2023**, *14*, 1038039. [CrossRef]
14. Kim, J.; Joo, J.H.; Kim, J.; Rim, H.; Shin, J.Y.; Choi, Y.-H.; Min, K.; Lee, S.Y.; Jun, S.-H.; Kang, N.-G. Platycladus Orientalis Leaf Extract Promotes Hair Growth via Non-Receptor Tyrosine Kinase ACK1 Activation. *Curr. Issues Mol. Biol.* **2024**, *46*, 11207–11219. [CrossRef] [PubMed]
15. Gao, Y.; Hu, M.; Meng, W.; Wen, W.; Zhang, P.; Fan, B.; Wang, F.; Li, S. Study on the Quality of Soybean Proteins Fermented by Bacillus Subtilis BSNK-5: Insights into Nutritional, Functional, Safety, and Flavor Properties. *Food Chem.* **2024**, *443*, 138523. [CrossRef]
16. Li, Q.; Zhu, H.; Hou, R.; Jiang, T.; Li, J.; Yan, X.; Wang, J. Microbial Fermentation Potentiates the Multifunctional Skin-Care Activities of *Polianthes tuberosa* L. Flower Extract: Antioxidant, Anti-Glycation, and Anti-Melanogenic Effects. *Cosmetics* **2025**, *12*, 243. [CrossRef]
17. Šelo, G.; Planinić, M.; Tišma, M.; Klarić, A.-M.; Bucić-Kojić, A. Effects of Fungal Solid-State Fermentation on the Profile of Phenolic Compounds and on the Nutritional Properties of Grape Pomace. *Microorganisms* **2024**, *12*, 1310. [CrossRef]
18. Matthews, H.K.; Bertoli, C.; De Bruin, R.A.M. Cell Cycle Control in Cancer. *Nat. Rev. Mol. Cell Biol.* **2022**, *23*, 74–88. [CrossRef]
19. Crowley, L.C.; Chojnowski, G.; Waterhouse, N.J. Measuring the DNA Content of Cells in Apoptosis and at Different Cell-Cycle Stages by Propidium Iodide Staining and Flow Cytometry. *Cold Spring Harb. Protoc.* **2016**, *2016*, pdb.prot087247. [CrossRef]
20. Yaseen, N.Q.; Qasim, Q.A.; Al-Tameemi, F.F. Study the Effect of Inflammatory Cytokines on Hair Loss. *Egypt. J. Med. Microbiol.* **2025**, *273*, 1505. [CrossRef]
21. Ru, Q.; Huang, K.; Yu, R.; Wu, X.; Shen, J. Effects of Camellia Oleifera Seed Shell Polyphenols and 1,3,6-Tri-O-Galloylglucose on Androgenic Alopecia via Inhibiting 5a-Reductase and Regulating Wnt/β-Catenin Pathway. *Fitoterapia* **2024**, *177*, 106116. [CrossRef]
22. Shin, D.W. The Molecular Mechanism of Natural Products Activating Wnt/β-Catenin Signaling Pathway for Improving Hair Loss. *Life* **2022**, *12*, 1856. [CrossRef]
23. Bellani, D.; Patil, R.; Prabhughate, A.; Shahare, R.; Gold, M.; Kapoor, R.; Shome, D. Pathophysiological Mechanisms of Hair Follicle Regeneration and Potential Therapeutic Strategies. *Stem Cell Res. Ther.* **2025**, *16*, 302. [CrossRef] [PubMed]

24. Jolliffe, I.T.; Cadima, J. Principal Component Analysis: A Review and Recent Developments. *Philos. Trans. R. Soc. Math. Phys. Eng. Sci.* **2016**, *374*, 20150202. [CrossRef]
25. Shen, N.; Wang, T.; Gan, Q.; Liu, S.; Wang, L.; Jin, B. Plant Flavonoids: Classification, Distribution, Biosynthesis, and Antioxidant Activity. *Food Chem.* **2022**, *383*, 132531. [CrossRef] [PubMed]
26. Liu, Y.; Zhu, J.; Liu, Z.; Zhi, Y.; Mei, C.; Wang, H. Flavonoids as Promising Natural Compounds for Combating Bacterial Infections. *Int. J. Mol. Sci.* **2025**, *26*, 2455. [CrossRef] [PubMed]
27. Wu, G. (Ed.) *Recent Advances in Animal Nutrition and Metabolism*; Advances in Experimental Medicine and Biology; Springer International Publishing: Cham, Switzerland, 2022; Volume 1354, ISBN 978-3-030-85685-4.
28. Kusaba, Y.; Fujimaru, Y.; Yamamoto, Y.; Kitagaki, H.; Jannatul, F. Methionine and Glycine Stabilize Mitochondrial Activity in Sake Yeast During Ethanol Fermentation. *Food Technol. Biotechnol.* **2019**, *57*, 535–543. [CrossRef]
29. Chidi, B.S.; Bauer, F.F.; Rossouw, D. The Impact of Changes in Environmental Conditions on Organic Acid Production by Commercial Wine Yeast Strains. *S. Afr. J. Enol. Vitic.* **2018**, *39*, 297–304. [CrossRef]

Disclaimer/Publisher's Note: The statements, opinions and data contained in all publications are solely those of the individual author(s) and contributor(s) and not of MDPI and/or the editor(s). MDPI and/or the editor(s) disclaim responsibility for any injury to people or property resulting from any ideas, methods, instructions or products referred to in the content.